Decoding the control of food intake

Insights from the habenula and hypothalamus

Slomp, M.

Publication date
2024

3

DISRUPTION OF LATERAL HYPOTHALAMIC CALORIE DETECTION BY A FREE CHOICE HIGH FAT DIET

Laura L.Koekkoek*, Margo Slomp*, Julien Castel,
Michael Mutersbaugh†, Ian Linville, Mireille J. Serlie,
Serge H. Luquet, Susanne E. la Fleur

* these authors contributed equally
† author deceased

The FASEB Journal, 2021, 35.9:e21804

Abstract

During the last few decades, the consumption of low-calorie sweeteners, as a substitute for caloric sweeteners, has sharply increased. Although research shows that caloric versus low-calorie sweeteners can have differential effects on the brain, it is unknown which neuronal populations are responsible for detecting the difference between the two types of sweetener. Using *in vivo* two-photon calcium imaging, we investigated how drinking sucrose or sucralose (a low-calorie sweetener) affects the activity of glutamatergic neurons in the lateral hypothalamus. Furthermore, we explored the consequences of consuming a free-choice high fat diet on the calorie detection abilities of these glutamatergic neurons. We found that glutamatergic neurons indeed can discriminate sucrose from water and sucralose, and that consumption of a free-choice high fat diet shifts the glutamatergic neuronal response from sucrose-specific to sucralose-specific, thereby disrupting calorie detection. These results highlight the disruptive effects of a diet high in saturated fat on calorie detection in the lateral hypothalamus.

Introduction

Consumption of sugar-sweetened beverages is a strong contributing factor to the development of obesity. [1] As an alternative, sugar is often replaced by low-calorie sweeteners, but there has been an ongoing debate about the health benefits of these sweeteners as a substitute. While caloric and low-calorie sweeteners provide an equivalent sweet taste, there is a body of contradictory evidence on how low-calorie sweeteners affect energy metabolism and weight gain. [2,3] The brain is a key mediator of these effects, and thus further understanding of how low-calorie sweeteners affect the brain is needed. Caloric and low-calorie sweeteners differentially activate brain reward areas. [4-6] However, it is unlikely that these reward areas directly sense the difference between caloric and low-calorie sweeteners, and it is yet to be determined which brain area conveys this information.

One prime candidate is the lateral hypothalamus (LH), which contains neurons sensitive to tasting sweet stimuli [7] and can modulate the preference for sweeteners. [8] Furthermore, it integrates energy-related signals from other hypothalamic nuclei [9], and conveys this information to reward related brain areas. [10] The two main neuronal populations of the LH are glutamatergic and GABAergic neurons [11], but only glutamatergic neurons play a role in taste preference. [9] It is unknown however, what the role of glutamatergic LH neurons is in detecting the difference between caloric and low-calorie sweeteners.

In addition to a lack of knowledge on which neural populations detect the presence of calories in different type of sweeteners, little is known about how other dietary factors, such as saturated fat consumption, can affect the neural response to sweeteners. We hypothesize that fat intake will affect calorie detecting abilities, as high fat diet feeding influences general LH neuronal activity. [12,13] Furthermore, the response of LH glutamatergic neurons to sucrose in mice is also altered by the consumption of a high fat diet. [13] It is unknown however, whether high fat diet feeding also affects calorie detection.

In this study, we assessed the effects of water, sucrose, and sucralose drinking on the activity of glutamatergic LH neurons using *in vivo* two-photon microscopy, thereby testing their calorie detecting abilities. Furthermore, we tested whether two-week consumption of a high fat diet affected the neuronal response to a caloric or low-calorie sweetener.

Methods

Animals

All experimental protocols were conducted in accordance with U.S. National Institutes of Health Guidelines for the Care and Use of Laboratory Animals and with the approval of the National Institute on Drug Abuse Animal Care and Use Committee. Two to four-month-old male and female heterozygous *Vglut2^{IREScre}* (RRID:IMSR_JAX:016963; C57BL/6J

background, Stock 16963, The Jackson Laboratory, Bar Harbor, ME, USA) mice were used in this study. Prior to stereotaxic surgery, mice were group housed with littermates in temperature- and humidity-controlled rooms with *ad libitum* access to water and rodent chow (PicoLab Rodent Diet 20, 5053 tablet, LabDiet/Land O'Lakes Inc., Saint Paul, MO, USA) on a 12 h light/dark cycle. Sucrose/sucralose preference testing was performed at the University Paris Diderot, and thus with approval of the Animal Care Committee of the University Paris Diderot-Paris 7 (CEB-25-2016).

Stereotaxic viral injection and GRIN lens implantation

For viral injection and Gradient Index (GRIN) lens implantation surgeries, mice were anesthetized with isoflurane and placed onto a stereotaxic apparatus (David Kopf Instruments, Tujunga, CA, USA). After exposing the skull by a minor incision, a small hole (< 1 mm diameter) was drilled for virus injection and subsequent GRIN lens implantation. First, a beveled 25-gauge needle was inserted into the hole to create a guide path for the lens (needle: bregma, -1.55 mm; midline, +0.90 mm; dorsal surface, -5.15 mm). Next, an adeno-associated virus (rAAV2.9/CAG.FLEX-GCaMP6s.WPRE.SV40, titer: 1.34×10^{13} genomic copies/ml; RRID:Addgene_100842; University of Pennsylvania Gene Therapy Program Vector Core, PA, USA) was injected (100 nl; rate: 30 nl/min) into the lateral hypothalamus (injection: bregma, -1.55 mm; midline, +0.90 mm; dorsal surface, -5.30 mm) by a pulled glass pipette (20-30 µm inner diameter) with a micromanipulator (Narishige International USA Inc., Amityville, NY, USA) controlling the injection speed. After injection, a GRIN lens (ILW-050-P146-055-NC; Go!Foton Corporation, NJ, USA) was lowered into position above the injection site (lens: bregma, -1.55 mm; midline, +0.90 mm; dorsal surface, -5.18 mm). A head bar was attached to the skull surface with cyanoacrylate and dental cement (C&B Metabond Adhesive Cement, Parkell Inc., Brentwood, NY, USA) was spread around the lens and inside the head bar to hold everything in place. A final layer of black dental cement (Contemporary Ortho-Jet, Lang Dental Manufacturing Company Inc., Wheeling, IL, USA) was applied around the lens on top of the previous layer of cement. A small piece of Parafilm was used to cover and protect the GRIN lens, and the inside of the head bar was filled with Kwik-Sil or Kwik-Cast (World Precision Instruments, Sarasota, FL, USA). After surgery, mice were individually housed for eight weeks for post-surgical recovery, inflammatory response reduction, and viral transduction.

Experimental paradigm

After the recovery period, mice were individually housed under reversed light dark conditions (lights off at 8 AM, on at 8 PM), and all imaging occurred in the dark period. After one week of acclimatization during which mice were handled daily, mice were assigned to one of two diets: the chow diet group (n = 6 in total (n = 3 female, n = 3 male)) received chow pellets (PicoLab Rodent Diet 20, 5053 tablet, LabDiet/Land O'Lakes Inc., Saint Paul, MO, USA) whereas the free choice high fat diet (fcHFD) group (n = 5 (n = 3 female, n = 2 male)) received chow pellets as well as a dish of pure beef tallow (Proper Foods For Life, Mesa, AZ, USA). Once started with

the diet, mice did not have access to a water bottle in their home cages, to ensure motivation for drinking in the imaging set-up. To prevent weight loss, the chow group received moist chow daily to facilitate eating and hydration (the beef tallow is hydrolyzed and fcHFD-fed animals therefore did not require moist chow). From the introduction of diet, mice were trained daily in the imaging set up to the imaging protocol. During second week of diet, mice underwent daily imaging sessions.

Two-photon fluorescence endomicroscopy system

We obtained images of LH^{VGLUT2} neurons across days using two-photon fluorescence endomicroscopy in awake, head-fixed mice. The GRIN lens has a working distance of approximately 130 µm on the object side. The numerical aperture (NA) was 0.5, which provides sufficient three-dimensional resolution for functional imaging of neuronal cell bodies and processes. The GRIN lens was incorporated into a two-photon fluorescence microscope equipped with a 10× air objective of 0.3 NA (Zeiss), which generated the initial focus of the excitation light to be relayed by the GRIN lens to the sample side. The two-photon fluorescence signal was collected and transported back to the microscope by the GRIN lens and detected with a photomultiplier tube (PMT; H7422; Hamamatsu Corporation, Bridgewater, NJ, USA). A Ti:Sapphire femtosecond oscillator (Mai Tai HP; Spectra-Physics, Milpitas, CA, USA) tuned to 910 nm was used as the excitation light source for all experiments. ScanImage 2017b (Vidrio Technologies LLC, Ashburn, VA, USA) was used to collect in vivo imaging recordings at 1.43 Hz for all mice. Laser power was set to 5-30%. For each mouse, the power setting was consistent among all recordings to avoid brain tissue damage by heat.

Imaging protocol

Mice were placed in the imaging rig in front of a custom-made lickometer that enabled the delivery of solutions and the measurement of licking using an infrared beam at the spout. After a three-minute baseline period, trials started. A trial commenced with a tone, followed by a 10 second window during which the mice could trigger a single delivery (0.0128 mL) by licking the spout, and ended with a 20 second window during which the mice could not trigger a delivery. Data are shown from the first six trials where a mouse triggered a delivery, as the large majority of mice triggered deliveries during the first six trials. As mice only had the opportunity to drink in the imaging set up, after the six trials used for analysis, they were allowed to continue triggering deliveries up to 60 deliveries to facilitate sufficient fluid intake. In total, mice underwent daily imaging sessions for nine subsequent days, three sessions in which water was delivered, three sessions in which a 10% sucrose solution was delivered, and three sessions in which a 1% sucralose solution was delivered. Because the chow-diet used contains small amounts of sucrose, we opted to always test the sucrose solution before the sucralose, as the mice were never sucrose-naïve. The first day of sucralose testing was not included in the analysis, as the lack of caloric content needs to be learned first [14,15]. On imaging days, food was removed for each individual mouse two hours before the onset of imaging.

Functional imaging analysis

To analyze the two photon calcium imaging data, the Calcium Imaging Analysis (CaImAn) package [16] and Non- Rigid Motion Correction (NoRMCorre) [17] package were used in MATLAB R2018A (The MathWorks Inc., Matick, MA, USA). First, imaging recordings were motion corrected using the NoRMCorre code. Next, using the CaImAn package's pipeline, regions of interest (ROI) were determined in the recordings using a constrained nonnegative matric factorization (CNMF) approach that finds the best spatial and temporal components explaining the observed fluorescence. This algorithm deals with heavily overlapping and neuropil contaminated movies, resulting in a background-corrected fluorescence signal per ROI. Recordings were manually aligned to ensure that the same ROI recorded throughout several days was noted to avoid artificially increasing the number of ROIs.

To improve the signal to noise ratio, the extracted fluorescence signal was preprocessed by smoothing using a moving mean. To determine the moving mean period, a moving mean of 1, 10, 20 and 50 frames was tested, and 20 frames resulted in optimal signal to noise ratio and was therefore used in preprocessing (**Supplemental Figure 2B**). After preprocessing the data, data were extracted from each delivery. A 5-frame window before the delivery was used as a baseline to calculate ΔF/F, and the response was measured in the 20 frames subsequent to the delivery. Deliveries with a negative baseline value were excluded from analysis. ROIs with any ΔF/F value > 5 (for LH^{VGLUT2} neurons) at any time point were consider outliers, and removed for subsequent analysis, eliminating ~ 1% of measurements. Data from multiple testing days were pooled. To group responses in "positive" "negative" and "no responders", we chose a change in ΔF/F of more than 0.2 as a threshold, based on earlier reports investigating lateral hypothalamic neuronal activity [13]. Therefore, neuronal responses showing an average increase in ΔF/F of more than 0.2 compared to baseline were classified as "positive", while an average decrease in ΔF/F more than 0.2 compared to baseline was classified as "negative". The remainder was classified as "no response". For determining the consistency of the response of an individual neuron, we assessed whether a positive or negative response was observed in over half (*i.e.* minimally 4 out of 6) of the trials per imaging session. Numbers of consistent neurons were then averaged across the multiple imaging sessions.

Histology

To confirm GRIN lens positioning, mice were deeply anesthetized with isoflurane and transcardially perfused with phosphate-buffered saline (1× PBS) followed by 4% paraformaldehyde (PFA) made with 1× PBS. Head bars and GRIN lenses were carefully removed to avoid damage to the brain tissue. Whole brains were removed and post-fixed in 4% PFA for 24 h at 4 °C and subsequently transferred to 30% sucrose made with 1× PBS for 2–5 days. Tissue samples were flash frozen and stored in a −80 °C freezer until further processing. Brains were sliced into 50-µm thick coronal sections using a cryostat (CM3050, Leica Biosystems Inc., Buffalo Grove, IL, USA). Sections were mounted with Fluoromount-G aqueous mounting

medium (Electron Microscopy Sciences, Hatfield, PA, USA) onto Superfrost Plus glass slides (VWR International, Monroeville, PA, USA) and coverslipped. Images were taken with an Axiozoom.V16 stereo zoom microscope (PlanNeoFluar Z 1x/NA0.25 objective with a 7x digital magnification; Carl Zeiss Microscpy LLC, NY, USA) using ZEN 2012 digital imaging software (RRID:SCR_013672). Locations of GRIN lenses were determined by the presence of lesions in the tissue (**Supplemental figure 1A**). Mice with lenses positioned outside of the lateral hypothalamus were excluded from the study (n = 2).

Preference test

To ensure that the sucralose concentration was iso-preferred to the sucrose solution, we performed a preference test in a separate group of mice. Four to six-month-old male and female heterozygous *Vglut2*^{IREScre} (RRID:IMSR_JAX:016963; C57BL/6J background, Stock 16963, The Jackson Laboratory, Bar Harbor, ME, USA [18]) mice were used in this study. Half the mice (n=6) received a chow diet (Safe A04 diet, Safe, Augy, France) the other half (n=6) received a fcHFD composed of the same chow pellets as well as a dish of pure beef tallow (Ossenwit/ Blanc de boeuf, Belgium). After two weeks of being on the diet, water bottles were removed overnight and the preference test was performed in the morning. Food was removed two hours before the preference test. During testing, mice had access to a bottle of 10% sucrose and a bottle of 1% sucralose for 40 minutes. Bottles were weighed after five minutes of access, as well as at the end of the test. Food and water were returned after testing. Sucrose and sucralose were equally preferred by both chow-fed and fcHFD-fed mice (**Supplemental Figure 1E**).

Statistical analysis

In order to analyze the interacting effects of the diet and the solution drunk during imaging, a mixed effects model was exploited using RStudio (https://rstudio.com/), running on R version 3.5.3 (the R Foundation, USA), using the *lme4* and *lmeTest* packages. The average fluorescence was taken as the dependent variable, and stimulus (water, sucrose, sucralose) were set as an independent fixed factor. Sex was included as a fixed factor to correct for male/female differences. To prevent artificially increasing the number of measurements, ROI number was set as a random effect to account for repeated measurements of the same ROI throughout multiple imaging sessions. This model was then ran on data from either chow-fed animals, or fcHFD-fed animals. To compare the positive or negative responses, the same mixed effects model was used, but only on the subset of data that included the positive or negative responses. The number of consistent neurons, or positive or negative responses was compared using a Chi-square test in Prism 8.3.0 (GraphPad Software, USA). To compare the number of positive or negative responses between stimuli, a Chi-square including only 2 stimuli was performed. For both the mixed effects model, and the Chi-square testing, a Bonferroni correction was applied to account for comparing the three stimuli and only p values below 0.0167 were accepted. For the daily caloric intake, a student's t-test was performed in Prism. For the body weight development, a repeated-measures ANOVA was performed in Prism. For the preference test, a two-way ANOVA was

performed in Prism. All bar and line graphs were created in Prism, while heatmaps were created in MATLAB. All data are plotted as mean ± SEM.

Results

fcHFD-feeding does not alter daily caloric intake or body weight

In order to specifically target glutamatergic LH neurons, mice expressing the CRE enzyme selectively in vesicular glutamate transporter 2 (VGLUT2) neurons were injected in the LH with a CRE-dependent virus (rAAV2.9/CAG.FLEX-GCaMP6s.WPRE.SV40.), causing specific expression of a calcium biosensor in LH^{VGLUT2} neurons. Next, a gradient index (GRIN) lens was implanted right above the injection site, allowing for visualization of calcium fluctuations as a proxy for LH^{VGLUT2} neuronal activity **(Figure 1A, B).** Mice were divided into two groups, a chow-fed group and a free-choice high fat diet (fcHFD)-fed group. During two weeks of diet, mice fed a fcHFD consumed approximately two thirds of their daily intake from fat, but

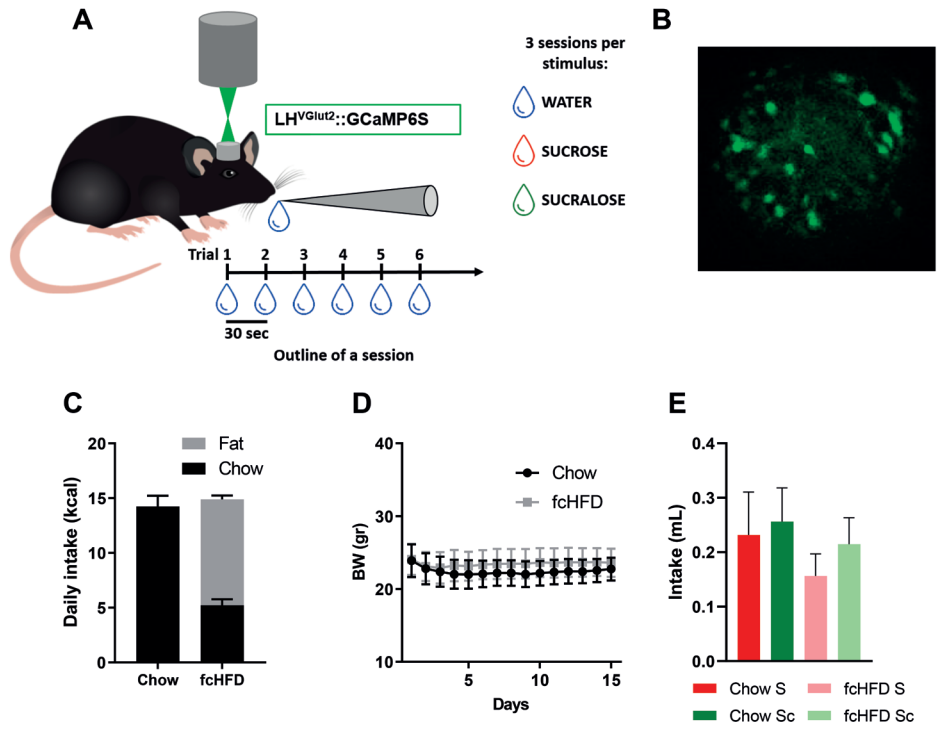

Figure 1. Mice fed a fcHFD consumed a similar amount of calories per day as chow-fed mice. **A.** Schematic of experimental design. **B.** Example field of view during imaging. **C.** Average daily caloric intake. **D.** Body weight progression during experiment. **E.** Sucrose versus sucralose consumption during 40 minute two-bottle preference test in chow-fed (n=6) and in fcHFD-fed (n=6) mice. No significant differences were found using a student's t-test (figure C), repeated measures ANOVA (figure D) or two-way ANOVA (figure E). Data are shown as mean ± SEM.

decreased their chow intake resulting in a total intake similar to chow-fed mice **(Figure 1C)**. Furthermore, body weight did not differ between chow-fed and fcHFD-fed mice **(Figure 1D)**. Changes in LH^{VGLUT2} neuronal activity were recorded in response to the consumption of water, sucrose, or sucralose **(Figure 1A)**. Sucrose and sucralose solutions were matched for equivalent sweetness, which was confirmed in a two-bottle preference test **(Figure 1E)**.

LH^{VGLUT2} neurons exhibit intrinsic variability in response to sucrose or sucralose consumption

We first assessed how many individual LH^{VGLUT2} neurons specifically respond to sucrose or sucralose consumption. An average increase in ΔF/F larger than 0.2 compared to baseline was considered a positive response, while an average decrease in ΔF/F larger than 0.2 compared to baseline was considered a negative response. Neurons were considered consistent if the positive or negative response was reproduced in more than half of the trials during one imaging session. Interestingly, we found only a very small subset of LH^{VGLUT2} neurons that consistently responded within one session to sucrose (3.26%-5.98% of measured neurons) or sucralose drinking (1.16%-5.85% of measured neurons), while the vast majority of neurons showed varying responses to sucrose or sucralose drinking **(Figure 2A, B)**. No neurons were found that showed a consistent response (to sucrose or sucralose) across sessions. Furthermore, diet-exposure had no significant effect on the number of consistently responding neurons.

Consumption of a fcHFD shifts the response of LH^{VGLUT2} neurons from sucrose to sucralose drinking

Next, we analyzed the LH^{VGLUT2} network response to water, sucrose or sucralose drinking. For this purpose, we combined all measurements (no distinction was made here for positive or negative responses) of LH^{VGLUT2} neurons that we obtained while mice were drinking water, sucrose or sucralose, but corrected for repeated measurements from the same neuron in our mixed effects model, to avoid artificially increasing the total number of measurements. In chow-fed mice, LH^{VGLUT2} neurons decrease their activity in response to sucrose, compared to water drinking **(Figure 3A, B)**. Furthermore, when mice drank the equivalent sweet sucralose, the response was similar as to water, confirming the calorie detecting abilities of LH^{VGLUT2} neurons **(Figure 3A, B)**. However, in fcHFD-fed mice, LH^{VGLUT2} neurons respond similarly to sucrose as compared to water, but markedly decreased their activity upon drinking sucralose **(Figure 3E, F, I)**. Thus, consumption of a fcHFD disrupts the calorie detecting abilities of these neurons.

Changes in average network ΔF/F are due to an altered number of neurons responding

We next aimed to further unravel the network dynamics that underlie the effects of sucrose or sucralose consumption on LH^{VGLUT2} activity. We again grouped responses into positive, negative and no responses based on an average change in ΔF/F larger than 0.2. Changes in average network ΔF/F can be due to two factors: (1) the number of positive or negative responses within

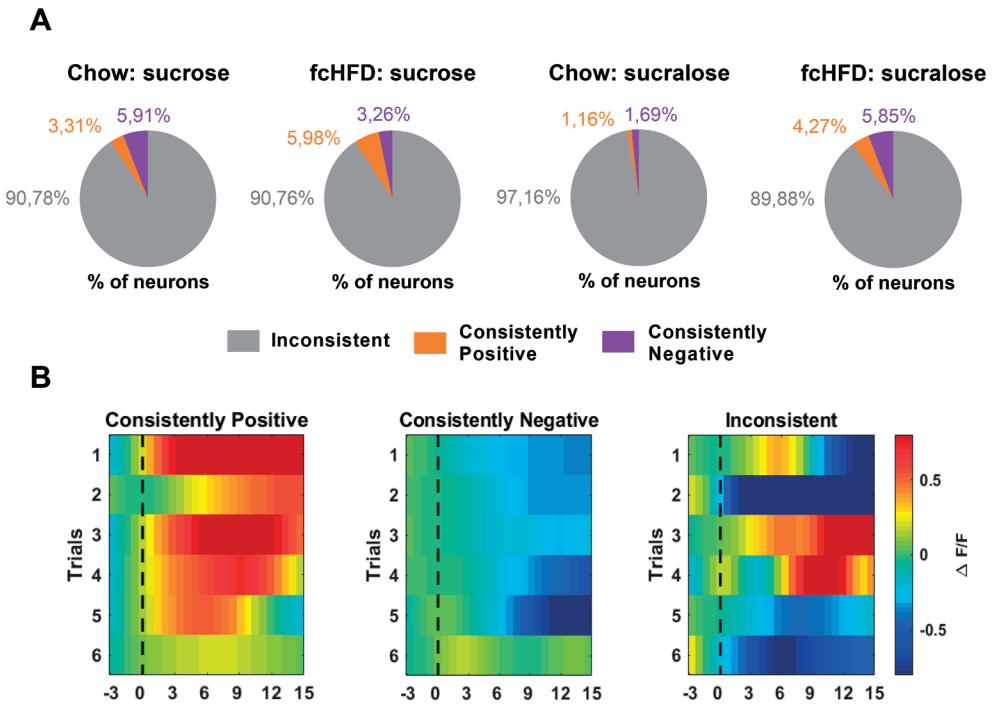

Figure 2. Individual LH^{VGLUT2} neurons show intrinsic variability in their response to sucrose or sucralose consumption. **A.** Percentages of neurons that were labelled as 'inconsistent' (i.e neurons that did not show a similar response in more than half of the trials), 'consistently positive' (i.e. neurons that showed an average increase in ΔF/F greater than 0.2 in more than half of the trials) and 'consistently negative' (i.e. neurons that showed an average decrease in ΔF/F greater than -0.2 in more than half of the trials), averaged across multiple imaging sessions testing sucrose or sucralose. **B.** Heatmaps showing examples of a 'consistently negative', a 'consistently positive' and an 'inconsistent' neuron.

the network and (2) the average magnitude of the positive or negative responses. For both chow-fed and fcHFD-fed mice, no significant changes in the average magnitude of the positive or negative responses were observed **(Table 1)**, indicating that changes seen in average network ΔF/F are due to a different number of neurons responding. Indeed, for chow-fed mice we found a significantly larger number of negative responses after sucrose drinking compared to water and sucralose drinking **(Figure 3C)**, and a slightly smaller number of positive responses **(Figure 3D)** (although this difference was only significantly different compared to sucralose drinking). For fcHFD-fed mice, a small significant increase in the number of negative responses after delivery of sucrose was observed **(Figure 3G)**, but this difference was not sufficient to alter the average network ΔF/F **(Figure 3E, F, I)**. Sucralose delivery on the other hand, induced a significantly larger increase in the number of negative responses in fcHFD-fed mice, as well as a sharp decrease in the number of positive responses **(Figure 3G, H)**, causing an overall decrease in average network ΔF/F **(Figure 3E, F, I)**. Thus, in conclusion, changes in the number,

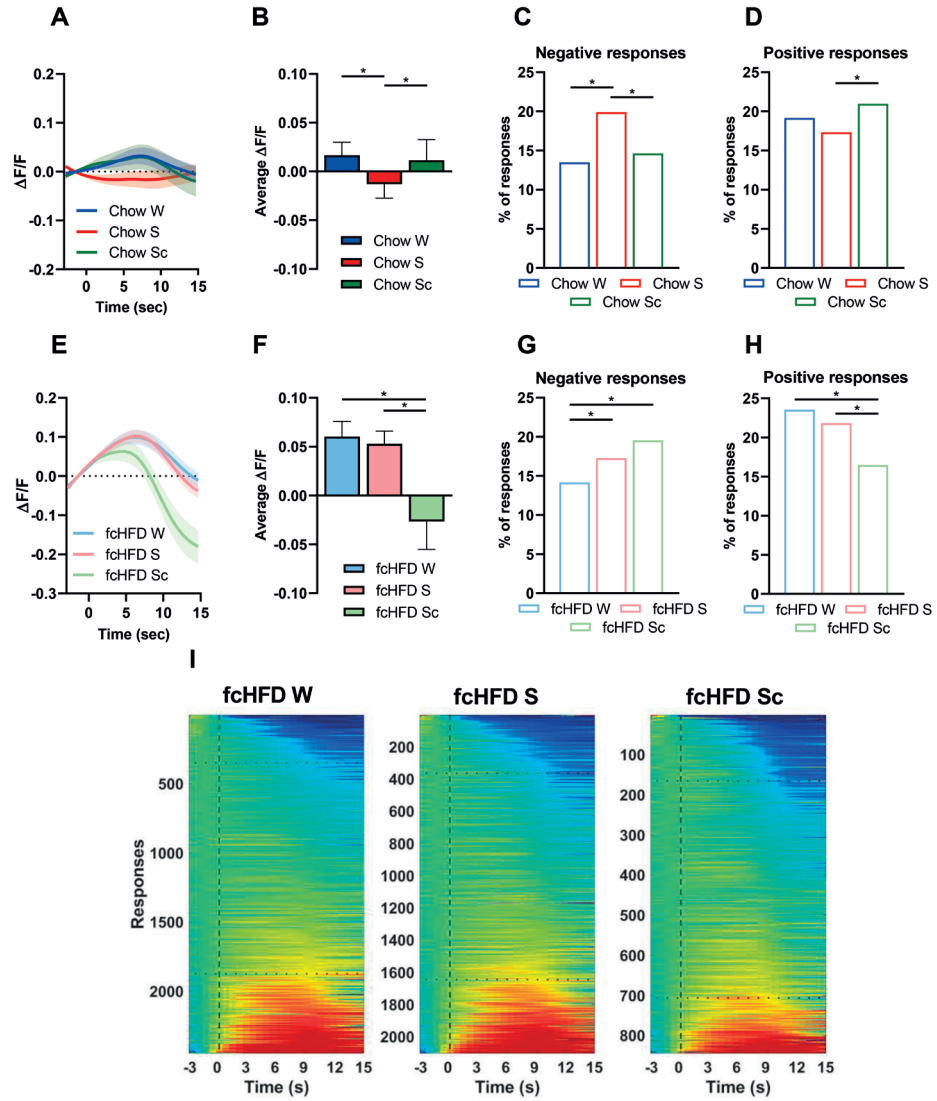

Figure 3. The network of LH^{VGLUT2} neurons is capable of calorie detection, but this is disrupted by fcHFD feeding. **A.** ΔF/F of all measured responses over time after solution delivery at t=0 in chow-fed mice. **B.** Average ΔF/F of all measured responses after delivery of water (W), sucrose (S) or sucralose (Sc) (chow W n=345 neurons, chow S n=315 neurons, chow Sc n= 213 neurons). **C.** Percentage of negative responses after delivery of water, sucrose or sucralose in chow-fed mice. **D.** Percentage of positive responses after delivery of water, sucrose or sucralose in chow-fed mice. **E.** ΔF/F over time after solution delivery at t=0 in fcHFD-fed mice. **F.** Average ΔF/F after delivery of water, sucrose or sucralose (fcHFD W n=285 neurons, fcHFD S n=246 neurons, fcHFD Sc n=193 neurons). **G.** Percentage of negative responses after delivery of water, sucrose or sucralose in fcHFD-fed mice. **H.** Percentage of positive responses after delivery of water, sucrose or sucralose in fcHFD-fed mice. **I.** Heatmaps showing ΔF/F after delivery of water, sucrose or sucralose at t=0 (dashed line), the dotted line represents the boundary for labeling a response 'positive' or 'negative'. Data shown as mean ± SEM. *= p<0.0167 as tested with a mixed effects model (figure B and F) or with a Chi-square test (figure C, D, G and H), for statistical outcomes see Supplemental Table 1.

Table 1. Average magnitude (ΔF/F) of all positive or all negative responses after water, sucrose or sucralose drinking[a].

	Chow-fed			fcHFD-fed		
	Water	**Sucrose**	**Sucralose**	**Water**	**Sucrose**	**Sucralose**
Positive Responses	0.523 ±0.0174	0.562 ±0.022	0.510 ±0.025	0.603 ±0.020	0.653 ±0.026	0.551 ±0.037
Negative Responses	-0.444 ±0.019	-0.442 ±0.015	-0.430 ±0.029	-0.434 ±0.017	-0.392 ±0.013	-0.422 ±0.032

[a]Data are shown as mean±SEM. No significant differences were observed using a mixed effects model, for statistics see Supplemental Table 1.

and not magnitude, of positive and negative responses underlie the observed average network ΔF/F changes in response to sucrose and sucralose drinking.

Discussion

In this study, we show that LH^{VGLUT2} neurons in chow-fed mice can discriminate sucrose from sucralose and water, indicating that these neurons sense the caloric value of sucrose. Moreover, consumption of a fcHFD affects the ability of LH^{VGLUT2} to discriminate sucrose from water, and shifts the LH^{VGLUT2} neuronal response from the calorie-containing sucrose, to the calorie-lacking sucralose.

We are the first to describe a neuronal population capable of detecting the caloric value of sucrose. Whether LH^{VGLUT2} neurons detect calories through direct glucose sensing [19], or through integration of signals from upstream neurons, will have to be further investigated. On the other hand, the downstream effects of various sweeteners have been previously described. For example, a body of evidence suggests that a critical difference between the consumption of caloric versus low-calorie sweeteners is the release of dopamine that is only associated with the consumption of caloric sweeteners. [4,5,20] Interestingly, a known downstream target of glutamatergic LH neurons are dopaminergic ventral tegmental area (VTA) neurons. As activation of LH^{VGLUT2} neurons that project to the VTA decreases dopamine release in the nucleus accumbens [10], a reduction in LH^{VGLUT2} activity seen only after sucrose intake might explain why sucrose consumption and not sucralose results in dopamine release.

In addition, we find that a fcHFD disrupts calorie detection by not only altering the response to sucrose, as was previously described in literature [13], but also by affecting the response to sucralose. While this may seem surprising, previous reports showed that consuming fat and low-calorie sweeteners has peripheral and central effects that are not elicited by consuming fat and a caloric sweetener. [21,22] For example, gut hormone release in response to a HFD containing a sucralose was significantly greater than in response to a HFD containing sucrose.

[21] Moreover, when subjects underwent functional MRI scanning while drinking a shake containing fat and sucralose, a different brain response was elicited than drinking a shake containing fat and glucose. [22] These findings, as well as our results, reflect a mismatch between sweet taste and caloric input, which is further exacerbated by the consumption of a fcHFD.

For the first time, we show that upon tasting the two sweeteners, LH^{VGLUT2} neurons discriminate sucrose from sucralose. This indicates that once the association between sweetener and lack of calories is established, oral taste signaling is sufficient to maintain this association, which is in line with previous findings. [23] Furthermore, despite equivalent sweetness, the two sweeteners have unique effects on oral taste signaling. These differences could be mediated through the sweet taste receptor components T1R2 and T1R3 that bind sucrose and sucralose with slightly different affinities [24] or through glucose transporters and ATP-dependent potassium channels expressed on oral taste cells that will specifically sense the presence of caloric sweeteners. [25-27]

Another striking feature of our findings, is that the effects of fcHFD-feeding on calorie detection are bodyweight independent, implicating that short-term exposure to saturated fat by itself is sufficient to alter and amplify the difference in neuronal response to caloric and low-calorie sweeteners, thereby possibly dysregulating feeding behavior before changes in bodyweight occur. Saturated fat can affect different stages of the neural processing of tasting sucrose or sucralose. For example, high fat diet feeding decreases the expression of the T1R3 component of the sweet taste receptor, thereby possibly affecting the oral taste signaling upon sucrose or sucralose drinking. [28] Alternatively, saturated fat intake could directly affect LH neuronal functioning, as LH neurons alter their reactivity in response to the presence of fatty acids. [29] Lastly fcHFD-feeding could alter the neural input to the LH. For example, dopamine-receptor 2 neurons in the nucleus accumbens have been identified as an important neuronal population for triglyceride-sensing, and can affect LH neuronal activity through projections that run via the ventral pallidum. [30]

A strong advantage of two-photon imaging is the ability to determine both the response of individual neurons, as well as the activity of the entire network, over subsequent trials. We show here that only a very small number of individual neurons maintains a similar response to sucrose drinking throughout multiple trials. Previous research has focused on quantifying the number of individual neurons responding specifically to sucrose consumption. [7,31,32] Comparable to our data, these previous papers found a limited number of these taste-specific neurons ranging from 3.5% [31], 5.8%[7] to 11% [32]. As a consequence of this low number of sucrose-specific neurons, it was not possible to compare the response to sucrose drinking of these individual neurons to water and sucralose drinking. Because we find a clear network response of LH^{VGLUT2} neurons to water, sucrose and sucralose drinking, we were able to compare network responses to the three solutions. Therefore, we propose to study both network dynamics in the future as well as the response of individual neurons.

LH^{VGLUT2} is a highly heterogeneous populations of neurons [11], and future research will thus have to unravel how these different subpopulations are involved in calorie detection. One subgroup of LH^{VGLUT2} neurons, the MCH neurons, play a role in calorie detection as ablation of these neurons alters the preference for sucrose versus sucralose [8], but this does not rule out the involvement of other subpopulations. For example, another subgroup of LH^{VGLUT2} neurons, the orexin neurons, responds to sucrose and sucralose consumption and modulates taste learning. [33,34] Future studies will further investigate whether these observed changes in glutamatergic network activity are due to an altered response by a specific subpopulation.

Furthermore, we found that changes in network activity are primarily due to an altered number of neurons responding. Specifically in chow-fed animals, we find that sucrose drinking increased the number of negative responses, suggesting that GABAergic input onto LH^{VGLUT2} neurons is possibly enhanced by sucrose drinking. An elegant study mapping the neural inputs onto MCH and orexin neurons, shows that both these subpopulations of LH glutamatergic neurons receive input from several brain areas involved in taste processing, including the thalamus, amygdala and insular cortex. [35] Interestingly, a strong GABAergic connection between MCH neurons and the amygdala, an area implicated with taste processing [36], was reported in this study. [35] Whether indeed GABAergic input from amygdala, or another taste-related brain area, is involved in the observed LH^{VGLUT2} response to sucrose drinking, remains to be determined.

To conclude, we find that glutamatergic LH neurons are capable of discriminating sucrose from water and sucralose, and that consumption of a fcHFD disrupts this calorie detection. We show a role for glutamatergic LH neurons in the brain's response to sweeteners, but also provide new evidence that consumption of a high fat diet can alter the neuronal response to sweeteners. Thus, these findings will aid in understanding how saturated fat intake impairs the brain's ability to detect calories and appropriately respond to different types of sweeteners.

References

1. Malik VS, Popkin BM, Bray GA, Despres JP, Hu FB. Sugar-sweetened beverages, obesity, type 2 diabetes mellitus, and cardiovascular disease risk. *Circulation.* 2010;121(11):1356-1364.
2. Fowler SPG. Low-calorie sweetener use and energy balance: Results from experimental studies in animals, and large-scale prospective studies in humans. *Physiol Behav.* 2016;164(Pt B):517-523.
3. Miller PE, Perez V. Low-calorie sweeteners and body weight and composition: a meta-analysis of randomized controlled trials and prospective cohort studies. *Am J Clin Nutr.* 2014;100(3):765-777.
4. Frank GK, Oberndorfer TA, Simmons AN, et al. Sucrose activates human taste pathways differently from artificial sweetener. *Neuroimage.* 2008;39(4):1559-1569.
5. Domingos AI, Vaynshteyn J, Voss HU, et al. Leptin regulates the reward value of nutrient. *Nat Neurosci.* 2011;14(12):1562-1568.
6. van Opstal AM, Kaal I, van den Berg-Huysmans AA, et al. Dietary sugars and non-caloric sweeteners elicit different homeostatic and hedonic responses in the brain. *Nutrition.* 2019;60:80-86.
7. Norgren R. Gustatory responses in the hypothalamus. *Brain Res.* 1970;21(1):63-77.
8. Domingos AI, Sordillo A, Dietrich MO, et al. Hypothalamic melanin concentrating hormone neurons communicate the nutrient value of sugar. *Elife.* 2013;2:e01462.
9. Fu O, Iwai Y, Narukawa M, et al. Hypothalamic neuronal circuits regulating hunger-induced taste modification. *Nat Commun.* 2019;10(1):4560.
10. Nieh EH, Vander Weele CM, Matthews GA, et al. Inhibitory Input from the Lateral Hypothalamus to the Ventral Tegmental Area Disinhibits Dopamine Neurons and Promotes Behavioral Activation. *Neuron.* 2016;90(6):1286-1298.
11. Mickelsen LE, Bolisetty M, Chimileski BR, et al. Single-cell transcriptomic analysis of the lateral hypothalamic area reveals molecularly distinct populations of inhibitory and excitatory neurons. *Nat Neurosci.* 2019;22(4):642-656.
12. Xin X, Storlien LH, Huang XF. Hypothalamic c-fos-like immunoreactivity in high-fat diet-induced obese and resistant mice. *Brain Res Bull.* 2000;52(4):235-242.
13. Rossi MA, Basiri ML, McHenry JA, et al. Obesity remodels activity and transcriptional state of a lateral hypothalamic brake on feeding. *Science.* 2019;364(6447):1271-1274.
14. Birch LL, McPhee L, Steinberg L, Sullivan S. Conditioned flavor preferences in young children. *Physiol Behav.* 1990;47(3):501-505.
15. Sclafani A, Zukerman S, Ackroff K. Postoral glucose sensing, not caloric content, determines sugar reward in C57BL/6J mice. *Chem Senses.* 2015;40(4):245-258.
16. Pnevmatikakis EA, Soudry D, Gao Y, et al. Simultaneous denoising, deconvolution, and demixing of calcium imaging data. *Neuron.* 2016;89(2):285-299.
17. Pnevmatikakis EA, Giovannucci A. NoRMCorre: An online algorithm for piecewise rigid motion correction of calcium imaging data. *Journal of neuroscience methods.* 2017;291:83-94.
18. Vong L, Ye C, Yang Z, Choi B, Chua S, Jr., Lowell BB. Leptin action on GABAergic neurons prevents obesity and reduces inhibitory tone to POMC neurons. *Neuron.* 2011;71(1):142-154.
19. Burdakov D, Gerasimenko O, Verkhratsky A. Physiological changes in glucose differentially modulate the excitability of hypothalamic melanin-concentrating hormone and orexin neurons in situ. *J Neurosci.* 2005;25(9):2429-2433.
20. Sclafani A, Touzani K, Bodnar RJ. Dopamine and learned food preferences. *Physiol Behav.* 2011;104(1):64-68.

21. Sanchez-Tapia M, Martinez-Medina J, Tovar AR, Torres N. Natural and Artificial Sweeteners and High Fat Diet Modify Differential Taste Receptors, Insulin, and TLR4-Mediated Inflammatory Pathways in Adipose Tissues of Rats. *Nutrients.* 2019;11(4).
22. Van Opstal AM, Hafkemeijer A, van den Berg-Huysmans AA, et al. Brain activity and connectivity changes in response to nutritive natural sugars, non-nutritive natural sugar replacements and artificial sweeteners. *Nutr Neurosci.* 2019:1-11.
23. Bonacchi KB, Ackroff K, Sclafani A. Sucrose taste but not Polycose taste conditions flavor preferences in rats. *Physiol Behav.* 2008;95(1-2):235-244.
24. Nie Y, Vigues S, Hobbs JR, Conn GL, Munger SD. Distinct contributions of T1R2 and T1R3 taste receptor subunits to the detection of sweet stimuli. *Curr Biol.* 2005;15(21):1948-1952.
25. Yee KK, Sukumaran SK, Kotha R, Gilbertson TA, Margolskee RF. Glucose transporters and ATP-gated K+ (KATP) metabolic sensors are present in type 1 taste receptor 3 (T1r3)-expressing taste cells. *Proc Natl Acad Sci U S A.* 2011;108(13):5431-5436.
26. Toyono T, Seta Y, Kataoka S, Oda M, Toyoshima K. Differential expression of the glucose transporters in mouse gustatory papillae. *Cell Tissue Res.* 2011;345(2):243-252.
27. Merigo F, Benati D, Cristofoletti M, Osculati F, Sbarbati A. Glucose transporters are expressed in taste receptor cells. *J Anat.* 2011;219(2):243-252.
28. Zhang XJ, Wang YQ, Long Y, et al. Alteration of sweet taste in high-fat diet induced obese rats after 4 weeks treatment with exenatide. *Peptides.* 2013;47:115-123.
29. Oomura Y, Nakamura T, Sugimori M, Yamada Y. Effect of free fatty acid on the rat lateral hypothalamic neurons. *Physiol Behav.* 1975;14(04):483-486.
30. Berland C, Montalban E, Perrin E, et al. Circulating Triglycerides Gate Dopamine-Associated Behaviors through DRD2-Expressing Neurons. *Cell Metab.* 2020;31(4):773-790 e711.
31. Yamamoto T, Matsuo R, Kiyomitsu Y, Kitamura R. Response properties of lateral hypothalamic neurons during ingestive behavior with special reference to licking of various taste solutions. *Brain Res.* 1989;481(2):286-297.
32. Li JX, Yoshida T, Monk KJ, Katz DB. Lateral hypothalamus contains two types of palatability-related taste responses with distinct dynamics. *J Neurosci.* 2013;33(22):9462-9473.
33. Gonzalez JA, Jensen LT, Iordanidou P, Strom M, Fugger L, Burdakov D. Inhibitory Interplay between Orexin Neurons and Eating. *Curr Biol.* 2016;26(18):2486-2491.
34. Mediavilla C, Cabello V, Risco S. SB-334867-A, a selective orexin-1 receptor antagonist, enhances taste aversion learning and blocks taste preference learning in rats. *Pharmacol Biochem Behav.* 2011;98(3):385-391.
35. Gonzalez JA, Iordanidou P, Strom M, Adamantidis A, Burdakov D. Awake dynamics and brain-wide direct inputs of hypothalamic MCH and orexin networks. *Nat Commun.* 2016;7:11395.
36. Kadohisa M, Rolls ET, Verhagen JV. Neuronal representations of stimuli in the mouth: the primate insular taste cortex, orbitofrontal cortex and amygdala. *Chem Senses.* 2005;30(5):401-419.

Appendices

Supplemental Table 1. Statistical outcomes for mixed effects model[a].

	Water vs. Sucrose			Water vs. Sucralose			Sucrose vs. Sucralose		
	p-value	**df**	**t-value**	**p-value**	**df**	**t-value**	**p-value**	**df**	**t-value**
Chow: Average network	**0.0013**	4388.4	-3.218	0.9008	3783.1	-0.125	**0.0138**	3783.1	-0.125
Chow: Positive responses	0.0191	1234.5	2.3462	0.3898	1216.2	0.8603	0.4355	1216.2	0.860
Chow: Negative responses	0.4832	1083.5	0.7014	0.2766	1098.5	1.0886	0.7340	1098.5	1.089
fcHFD: Average network	0.8975	4019.1	0.129	**0.00001**	3012.8	-4.451	**0.0000**	3012.8	-4.401
fcHFD: Positive responses	0.0466	1147.4	1.9922	0.2775	1078.3	-1.087	**0.0480**	1078.3	-1.087
fcHFD: Negative responses	0.1289	872.6	1.5201	0.8256	804.4	0.2205	0.8250	804.4	0.220

[a]Bonferroni correction was applied and only p-values below 0.0167 were accepted.

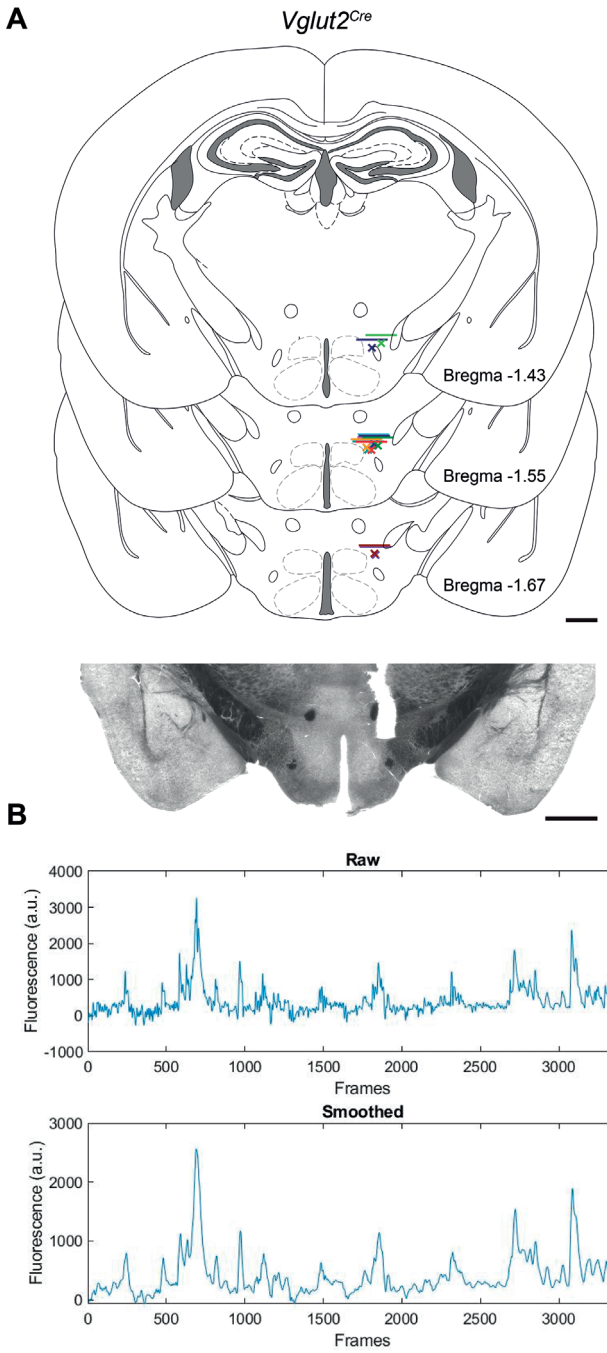

Supplemental figure 1. **A.** Placement of lenses for mice included in this study and representative darkfield images from each mouse line demonstrating lens placement. Lines indicate bottom of the lens and ×'s indicate working distance (approx. 130 µm). Scale bar schematics = 500 µm; Scale bar representative images = 1 mm **B.** Example trace of the raw fluorescence (top) and fluorescence after smoothing (bottom) of a single neuron.